

# $\alpha 3\alpha 5\beta 2$ -Nicotinic Acetylcholine Receptor Contributes to the Wound Repair of the Respiratory Epithelium by Modulating Intracellular Calcium in Migrating Cells

Jean-Marie Tournier,\* Kamel Maouche,\*  
Christelle Coraux,\* Jean-Marie Zahm,\*  
Isabelle Cloëz-Tayarani,<sup>†</sup>  
Béatrice Nawrocki-Raby,\* Arnaud Bonnomet,\*  
Henriette Burlet,\* François Lebagry,\*<sup>‡</sup>  
Myriam Polette,\*<sup>§</sup> and Philippe Birembaut\*<sup>§</sup>

From INSERM UMRS-514,\* IFR53, Université de Reims, Reims;  
Unité de Biologie Cellulaire,<sup>§</sup> Laboratoire Pol Bouin, and Service  
de Pneumologie,<sup>‡</sup> CHU de Reims, Reims; and Unité Récepteurs et  
Cognition,<sup>†</sup> CNRS URA-2182, Institut Pasteur Paris, Paris, France

**Nicotinic acetylcholine receptors (nAChRs), present in human bronchial epithelial cells (HBECs), have been shown *in vitro* to modulate cell shape. Because cell spreading and migration are important mechanisms involved in the repair of the bronchial epithelium, we investigated the potential role of nAChRs in the wound repair of the bronchial epithelium. *In vivo* and *in vitro*,  $\alpha 3\alpha 5\beta 2$ -nAChRs accumulated in migrating HBECs involved in repairing a wound, whereas  $\alpha 7$ -nAChRs were predominantly observed in stationary confluent cells. Wound repair was improved in the presence of nAChR agonists, nicotine, and acetylcholine, and delayed in the presence of  $\alpha 3\beta 2$  neuronal nAChR antagonists, mecamylamine,  $\alpha$ -conotoxin MII, and  $\kappa$ -bungarotoxin;  $\alpha$ -bungarotoxin, an antagonist of  $\alpha 7$ -nAChR, had no effect. Addition of nicotine to a repairing wound resulted in a dose-dependent transient increase of intracellular calcium in migrating cells that line the wound edge. Mecamylamine and  $\kappa$ -bungarotoxin inhibited both the cell-migration speed and the nicotine-induced intracellular calcium increase in wound-repairing migrating cells *in vitro*. On the contrary  $\alpha$ -bungarotoxin had no significant effect on migrating cells. These results suggest that  $\alpha 3\alpha 5\beta 2$ -nAChRs actively contribute to the wound repair process of the respiratory epithelium**

**by modulating intracellular calcium in wound-repairing migrating cells. (Am J Pathol 2006; 168:55–68; DOI: 10.2353/ajpath.2006.050333)**

Because it is permanently exposed to airborne pollutants, the airway epithelium can be locally injured and remodeled. *In vivo* and *in vitro* models of airway epithelial injury and wound repair have shown that the spread and migration of poorly differentiated epithelial cells neighboring the wound margin are the first major events in the wound repair process, allowing the recovery of the denuded extracellular matrix.<sup>1,2</sup> Cell migration is essential for the rapid reconstitution of a cohesive epithelial structure. Indeed, rapidly after migrating cells have covered the denuded wounded area, the barrier integrity of the bronchial epithelium is restored.<sup>3</sup>

Among the numerous cellular and molecular factors involved in cell migration, nicotinic acetylcholine receptors (nAChRs) have been shown to positively or negatively regulate cell migration. The nAChRs are a family of ionotropic receptor proteins formed by five  $\alpha/\beta$  homologous or five  $\alpha$  identical subunits.<sup>4</sup> Cells from the surface bronchial epithelium have been shown to contain  $\alpha 3$ ,  $\alpha 4$ ,  $\alpha 5$ ,  $\alpha 7$ ,  $\beta 2$ , and  $\beta 4$  subunits of nAChRs.<sup>5–8</sup> Patch-clamp experiments demonstrated that human bronchial epithelial cells (HBECs) in culture expressed functional nAChRs with ion-gating properties similar to those of nAChRs formed by  $\alpha 3$ ,  $\alpha 5$ , and  $\beta 2$  or  $\beta 4$  subunits, also referred to as the  $\alpha 3\beta 2$ -nAChRs.<sup>4,6</sup> In addition, HBECs express the  $\alpha 7$ -nAChR.<sup>7</sup> These nAChRs mediate the effects of endogenous acetylcholine (ACh) and exogenous nicotine.

Supported by grants from the Association pour la Recherche sur les Nicotianées, the Lions Club Villers-Cotterêts Soissons, the Association Vaincre La Mucoviscidose (to C.C.), and the Région Champagne-Ardenne (to A.B. and K.M.).

Accepted for publication August 26, 2005.

Address reprint requests to Jean-Marie Tournier, INSERM UMRS-514, 45 rue Cognacq-Jay, 51092 Reims Cedex, France. E-mail: jm.tournier@univ-reims.fr.

It is now established that ACh may function as an autocrine or paracrine signaling molecule in a variety of nonneuronal tissues.<sup>9,10</sup> ACh is synthesized and secreted by airway bronchial epithelial cells.<sup>8</sup> These cells contain all of the components for a nonneuronal autocrine/paracrine cholinergic loop: the choline high-affinity transporter, which allows choline to enter the cells; the enzyme choline acetyltransferase, which synthesizes ACh from free cytosolic choline and acetylcoenzyme A; and the vesicular ACh transporter, which packages ACh into vesicles in neurons<sup>11</sup> but whose role in HBECs remains to be established.<sup>8–10</sup> Cultures of HBECs also confirm the synthesis and secretion of ACh and the activity of cholinesterases that degrade ACh.<sup>8</sup>

ACh and/or nicotine regulate bronchial epithelial cell<sup>5,6</sup> and keratinocyte<sup>12,13</sup> adhesion; are chemotactic for pulmonary neutrophils,<sup>14</sup> vascular smooth muscle cells,<sup>15</sup> and spermatozoa;<sup>16</sup> regulate neurite outgrowth and motility;<sup>17,18</sup> inhibit keratinocyte<sup>19</sup> or cerebellar granule cell migration;<sup>20</sup> or have no effect on gastric epithelial cell<sup>21</sup> or breast carcinoma cell<sup>22</sup> migration. Different nAChRs may play opposing roles in nicotinic control of cell migration. For example,  $\alpha 3$ - and  $\alpha 7$ -nAChRs regulate keratinocyte chemokinesis and chemotaxis, respectively, with nicotine inhibiting random migration but stimulating directional migration.<sup>23</sup>

When exposed to mecamylamine, a noncompetitive nAChR antagonist that more efficiently blocks  $\alpha/\beta$  heteromers than  $\alpha 7$ -nAChR,<sup>24</sup> or to  $\kappa$ -bungarotoxin, a selective and slowly reversible antagonist of  $\alpha 3/\beta 2$ -nAChR,<sup>25</sup> HBECs in culture progressively shrink, detach their flat cytoplasmic extensions from the underlying extracellular matrix, and detach from neighboring cells, effects that are reversed after removing the antagonists from the culture medium.<sup>5,6</sup> Because of such findings and because modifications of cell-cell and cell-extracellular matrix contacts contribute to cell migration, we investigated the potential role of nAChRs during HBEC migration and wound repair of the human bronchial epithelium.

## Materials and Methods

### Source of Bronchial Tissue

Human bronchial tissues from patients (mean  $\pm$  SD; age,  $69 \pm 5$  years; range, 48 to 84 years) undergoing surgery for bronchial carcinoma were obtained from microscopically normal areas distant from the tumor. Immediately after excision, the samples were immersed in Ham F-12/Dulbecco's modified Eagle's medium (1/3, v/v) (Gibco BRL, Paisley, Scotland) supplemented with 100 U/ml penicillin, 100  $\mu$ g/ml streptomycin (Gibco), and 25  $\mu$ g/ml gentamicin (Sigma Aldrich Chimie, L'Isle d'Abeau Chesnes, France). Specimens were then either processed for cell isolation or for an *ex vivo* wound repair model.

### Cell Culture

HBECs were isolated and cultured as previously described with some modifications.<sup>26</sup> Briefly, the bronchial tissues were digested overnight at 4°C with 0.1% Pronase E, and dissociated cells were resuspended in culture medium, which consisted of Ham F-12/Dulbecco's modified Eagle's medium (1/3, v/v) supplemented with 0.87  $\mu$ mol/L bovine insulin, 65 nmol/L human transferrin, 1.6 nmol/L recombinant human epidermal growth factor, 1.38  $\mu$ mol/L hydrocortisone, 30 nmol/L retinyl acetate, 9.7 nmol/L 3,3',5-triiodo-L-thyronine, 2.7  $\mu$ mol/L (–)epinephrine, 35  $\mu$ g/ml bovine pituitary extract, 5  $\mu$ mol/L ethanolamine, 5  $\mu$ mol/L *o*-phosphorylethanolamine, 30 nmol/L sodium selenite, 1 nmol/L manganese chloride, 0.5  $\mu$ mol/L sodium metasilicate, 1 nmol/L ammonium molybdate, 5 nmol/L ammonium vanadate, 1 nmol/L nickel sulfate, 0.5 nmol/L stannous chloride, 100 U/ml penicillin, and 100  $\mu$ g/ml streptomycin (all reagents from Sigma), as previously described.<sup>27</sup> Isolated cells were either seeded on four-well Lab-Tek II chambered coverglasses (Nalge Nunc, Naperville, IL) to study cell migration or intracellular calcium on 12-well plates (Beckton Dickinson, Le Pont de Claix, France) to evaluate wound repair index, or on 18-mm glass coverslips (VWR Int., Fontenay-sous-Bois, France) for immunocytochemistry. All culture surfaces were coated with rat tail type I collagen and prepared in the presence of 0.25  $\mu$ g/ml carbodiimide as previously described.<sup>26</sup> Fetal calf serum (10%) was added to the culture medium during the first 15 hours after seeding to facilitate cell adhesion. Cells were cultured at 37°C in a humidified incubator in the presence of 5% CO<sub>2</sub> and 95% air. Confluent primary cultures of HBECs were generally obtained after 1 to 2 days.

### Wound Repair Models

#### In Vitro Wound Repair Model

Primary cultures of confluent HBECs were locally injured by depositing a 1- $\mu$ l drop of 1 mol/L sodium hydroxide at the center of the culture as previously described.<sup>26</sup> Sodium hydroxide was rapidly neutralized with phosphate-buffered saline (PBS) and a circular wound area of  $\sim 30$  mm<sup>2</sup> resulted from the sodium hydroxide-induced cellular lysis. Evolution of the remaining surface of the wound area was examined every day with an SMZ-U binocular microscope (Nikon France, Champigny-sur-Marne, France), and the corresponding wound area was calculated using a graphic table and the Scion Image software program (National Institutes of Health, Bethesda, MD). The linear relationship between the wound surface and time was used to calculate a wound repair index, corresponding to the decrease in wound surface per hour. When the wound had repaired 30 to 60% of its initial surface (1 to 2 days), cultures were then processed for the measurement of cell migration, intracellular calcium concentration, or immunofluorescence labeling studies as follows. Before fixation, HBEC cultures were rapidly washed in PBS. Cultures were then either fixed for 10 minutes in methanol at –20°C or se-

quentially fixed for 5 minutes in 3.7% paraformaldehyde in PBS, washed in PBS, incubated for 5 minutes in 0.1 mol/L glycine in PBS, washed in PBS, permeabilized for 1 minute with 0.5% Triton X-100, rinsed in PBS, and stored at 4°C until used.

### **Ex Vivo Wound Repair Model**

Freshly collected human bronchial tissue samples, ~10 × 10 mm, were locally injured with a metallic probe (2 mm in diameter), frozen with liquid nitrogen, and applied for 10 seconds to the tissue sample with a calibrated pressure of 33 kPa. Under these conditions, only cells of the surface epithelium were damaged and desquamated. In a previous study, we observed that the basement membrane in the wound area remains intact, as demonstrated by the presence of immunoreactive laminin and type IV collagen as a continuous thin layer in the damaged area.<sup>28</sup> After wound induction, tissue samples were maintained in culture for 1 to 2 days in culture medium. After 1 day in culture, the epithelial cells migrated to the wound edge to begin repair, appearing as flat cells.<sup>28,29</sup> At that time, cultures were fixed for 1 hour at 4°C in 4% paraformaldehyde in PBS, incubated 1 hour in 5% sucrose in PBS, 1 hour in 10% sucrose, 15 hours in 20% sucrose, embedded in Tissue Tek OCT compound (Sakura, Zoeterwoude, The Netherlands), and frozen in liquid nitrogen.

### **Cell Migration Quantification**

After wound induction, the wounded culture was placed in a small transparent culture chamber of an IM35 inverted microscope (Zeiss, Oberkochen, Germany). Phase contrast micrographs of repairing cultures focused at the wound edge were taken at regular intervals. The images were digitized as 512 × 512 pixels and 8-bit array using a Sparc-Classic (Sun Microsystems, Mountain View, CA) workstation equipped with an XVideo card (Parallax Graphics, Santa Clara, CA). Cell migration was quantified using a previously described software<sup>30</sup> with three main functions: the detection of cell nuclei, the computation of the trajectories of these nuclei, and the analysis of these trajectories. From the trajectory of each nucleus, the computer calculated the cell migration speed.

When analyzing the effect of nAChR agonists or antagonists (nicotine, ACh, mecamylamine, and  $\alpha$ -bungarotoxin from Sigma;  $\alpha$ -conotoxin MII synthesized by Genepex, Montpellier, France;  $\kappa$ -bungarotoxin from Biotaxon Inc., St. Cloud, France) on HBEC migration, we restricted migration assessment to a population of cells located close to the edge of the wound, ie, within a distance corresponding to approximately one to two cells starting from the edge of the wound. Indeed, we previously observed that cell migration speed progressively decreases as the distance of the cells from the wound edge increases.<sup>30</sup>

### **Immunocytochemistry**

Sections of frozen bronchial tissues were cut (5  $\mu$ m thick) at -20°C in a 2800 Frigocut cryostat (Cambridge Instruments, Nussloch, Germany) and transferred to gelatin-coated slides. Tissue sections and HBEC cultures undergoing repair were immunoreacted with specific polyclonal (Ab) or monoclonal (mAb) antibodies using an indirect immunofluorescence labeling technique. All incubations were conducted at room temperature.

The following antibodies were used to localize nAChR subunits and choline acetyltransferase in repairing bronchial tissues or HBEC cultures: rat mAb-210 ( $\alpha$ 1,3,5; 10  $\mu$ g/ml) mAb-268 ( $\alpha$ 5, 10  $\mu$ g/ml), and mAb-290 ( $\beta$ 2, 10  $\mu$ g/ml) from Sigma; mouse mAb-8A4 ( $\alpha$ 4, 1:40; Novocastra Laboratories, Newcastle on Tyne, UK); goat C-18-Ab ( $\alpha$ 3, 10  $\mu$ g/ml), D-19-Ab ( $\alpha$ 5, 10  $\mu$ g/ml), C-20-Ab ( $\beta$ 2, 5  $\mu$ g/ml), and rabbit H-302-Ab ( $\alpha$ 7, 10  $\mu$ g/ml), all from Santa Cruz Biotechnology, Santa Cruz, CA; and mouse mAb-5270 (choline acetyltransferase, 20  $\mu$ g/ml; Chemicon, Temecula, CA). Non-specific binding was blocked for 30 minutes with 3% bovine serum albumin (BSA) in PBS. The samples were then incubated for 60 minutes with the primary antibodies prepared in 1% BSA in PBS (PBS-BSA). After two washes in PBS for 5 minutes, and one wash in PBS-BSA for 5 minutes, the samples were incubated with biotinylated secondary antibodies (Jackson ImmunoResearch, West Grove, PA) diluted 1/100 in PBS-BSA for 60 minutes and then incubated with Alexa 488-streptavidin (Molecular Probes, Eugene, OR) diluted 1/50 in PBS for 30 minutes. We verified the absence of cross-reactivity by incubating control cultures and tissue sections with nonimmune IgG instead of the primary antibody. After immunolabeling, cultures were counterstained with Harris hematoxylin (Diagnostica Merck, Darmstadt, Germany) and mounted in Citifluor anti-fading solution (Agar Scientific, Essex, UK). All fluorescence-labeled preparations were examined with an Axiophot microscope (Zeiss) using successive epifluorescence and Nomarski differential interference illumination.

### **Identification of [<sup>125</sup>I]-Epibatidine Binding Sites in the Bronchial Epithelium**

Sections of frozen bronchial tissues were cut (20  $\mu$ m thick) at -20°C, transferred to SuperFrost Plus slides (Kindler, Freiburg, Germany), and kept at -20°C until use. Sections were incubated at room temperature with 200 pmol/L [<sup>125</sup>I]-epibatidine (specific activity 2200 Ci/mmol; Perkin Elmer, Boston, MA) in 50 mmol/L Tris, pH 7.4, for 30 minutes. After incubation, sections were rinsed twice for 5 minutes in the same buffer and briefly in ice-cold distilled water. Nonspecific binding was measured in the presence of 1 mmol/L nicotine. Sections were then exposed to Kodak Biomax films (Kodak Pathé, Paris, France) for 80 hours. Sections were stained using carbol toluidine blue (Réactifs RAL, Martillac, France).

## Reverse Transcriptase-Polymerase Chain Reaction (RT-PCR) Analyses

RNA was extracted from migrating HBECs with High Pure RNA isolation kit as recommended by the manufacturer (Roche Diagnostics GmbH, Mannheim, Germany). RNA concentrations were measured with the Ribogreen kit (Molecular Probes). RT-PCR was performed with 10 ng of total RNA by using the ThermoStable *rTth* Reverse Transcriptase RNA PCR kit (Applied Biosystems, Foster City, CA). Primers were designed to amplify specific members of the nAChR gene family using GenBank sequences or previously designed primers as mentioned. Their sequences and expected product size (in parentheses) were as follows:  $\alpha 3$ , 5'-AGCAACGAGGGCAACGCTCAGAA-3' and 5'-CAGAACTAGAGCTTCTCGTGAGGT-3' (195 bp);  $\alpha 4$ , 5'-TGGGTGAAGCAGGAGAGTGG-3' and 5'-AGTCCAGCTGGTCCACG-3' (346 bp);<sup>6</sup>  $\alpha 5$ , 5'-GTG-GTAGTGGACCAAAATCTTCTA-3' and 5'-GCCCAAGAGATCCAACAATTGAAA-3' (191 bp);  $\alpha 7$ , 5'-CAGTCT-TACTCTCTTACCGTCT-3' and 5'-GCACCAGTTCAGAGGATGACTC-3' (217 bp);  $\beta 2$ , 5'-CAGCTCATCAG-TGTGCA-3' and 5'-GTGCGGTCTAGGTCCA-3' (347 bp);<sup>12</sup> and  $\beta 4$ , 5'-TCGATGTGCCTCTCATCGGCAA-3' and 5'-GCTTGGTCACGCATGACTTGCT-3' (239 bp). All PCR products were verified by sequencing (SeqLab, Göttingen, Germany).

## Measurement of $[Ca^{2+}]_i$

The concentration of  $[Ca^{2+}]_i$  in migrating HBECs was measured with the calcium-sensitive Fura-2 acetoxymethyl ester by the fluorescence ratiometric method with modifications.<sup>5</sup> Cells were cultured in four-well Lab-Tek II chambered coverglasses, were loaded with 3  $\mu$ mol/L Fura-2 (Molecular Probes) in culture medium containing 20 mmol/L HEPES for 60 minutes, washed in the same medium, and allowed to recover in a 5% CO<sub>2</sub> incubator at 37°C for 60 minutes. The chamber slide was placed on the preheated stage (37°C) of an inverted Nikon TE300 microscope equipped with an incubator chamber. The Fura-2 fluorochrome was excited every 10 or 20 seconds and sequentially at wavelengths of 340 and 380 nm generated by a Polychrome II monochromator (TILL Photonics, Planegg, Germany); the emission at 510 nm was detected with a  $\times 40$  Plan Fluor objective (Nikon) and a cooled charge-coupled device camera (Micromax; Roper Scientific, Evry, France). In all experiments, increments of  $[Ca^{2+}]_i$  evoke a positive signal at 340 nm and a negative signal at 380 nm. The wavelengths of excitation and emission, the time course of image acquisition, and the image treatment were controlled by the computer software Metafluor (Universal Imaging, West Chester, PA). The fluorescence was quantified by averaging pixel intensities in the area of interest and by subtracting background fluorescence, corresponding to a wound area devoid of cells.

For  $[Ca^{2+}]_i$  calculations,  $R = F_{340}/F_{380}$ ,  $R_{min}$  (0% saturation of the dye with  $Ca^{2+}$ ) and  $R_{max}$  (100% sat-

uration with  $Ca^{2+}$ ) were determined. At the end of each acquisition,  $R_{max}$  was obtained by adding 5  $\mu$ mol/L ionomycin (Sigma) to the culture medium, and  $R_{min}$  was obtained after removing ionomycin, washing the cells with culture medium, and incubating the cells for 10 minutes in 5 mmol/L EGTA (Sigma).  $R$ ,  $R_{max}$ , and  $R_{min}$  were calculated from image acquisitions derived from the same group of cells and the same background area.  $[Ca^{2+}]_i$  was calculated with the following equation:  $[Ca^{2+}]_i = K_D \times F_{min}/F_{max} \times [(R - R_{min})/(R_{max} - R)]$ , where  $R$  is the fluorescent ratio,  $R_{max}$  is the maximum ratio value, and  $F_{max}$  is  $F_{380}$  measured at high  $[Ca^{2+}]_i$  in the presence of 5  $\mu$ mol/L ionomycin, and  $R_{min}$  is the minimum ratio value, and  $F_{min}$  is  $F_{380}$  measured at low  $[Ca^{2+}]_i$  in the presence of 5 mmol/L EGTA, and  $K_D$  is the dissociation constant of the  $Ca^{2+}$  binding to Fura-2 (224 nmol/L).<sup>31</sup>

## Immunoprecipitation and Western Blotting

Proteins in migrating HBECs present in cultures derived from four different bronchial samples were extracted in RIPA buffer [50 mmol/L Tris, pH 7.4, 150 mmol/L NaCl, 1% Igepal (v/v), 1% sodium deoxycholate (w/v), 0.1% sodium dodecylsulfate (w/v)] containing complete protease inhibitor cocktail (Roche Diagnostics GmbH, Mannheim, Germany). Lysates were pooled and cleared by spinning at 12,500  $\times g$  for 10 minutes. Protein concentrations were determined with the BCA protein assay reagent (Pierce, Rockford, IL). Proteins were preincubated with protein G-Sepharose CL-4B beads (Amersham Biosciences, Saclay, France) by rocking 1 hour at 4°C. These beads were discarded, and the supernatant (500  $\mu$ g protein) was incubated with 1  $\mu$ g of one of the following goat polyclonal nAChR-specific antibodies (C-18-Ab to  $\alpha 3$ , D-19-Ab to  $\alpha 5$ , or C-20-Ab to  $\beta 2$ ) or 1  $\mu$ g control IgG for 3 hours on a rotating wheel at 4°C. Protein G-Sepharose beads were then added, and the samples were incubated for 1 hour at 4°C. Beads were washed six times in lysis buffer and boiled in Laemmli sample buffer, and proteins were separated on 10% sodium dodecyl sulfate-polyacrylamide gel electrophoresis gels under reducing conditions using the Bio-Rad Mini-PROTEAN II electrophoresis system (Bio-Rad, Hercules, CA) and transferred to Immobilon polyvinylidene difluoride membrane (Millipore) using the Bio-Rad Mini Trans-Blot system. Blots were incubated for 1 hour in blocking buffer (5% low-fat milk powder, 0.1% Tween-20 in PBS) and then incubated overnight at 4°C with one of the following antibodies diluted in blocking buffer: mAb-210 ( $\alpha 1,3,5$ ), mAb-268 ( $\alpha 5$ ), or mAb-290 ( $\beta 2$ ). The membranes were incubated with a horseradish peroxidase-conjugated rabbit anti-rat antibody (DAKO, Glostrup, Denmark). Signal was detected with ECL+ kit (Amersham Biosciences) and quantified with a Las-1000+ camera (Raytest France, Courbevoie, France).



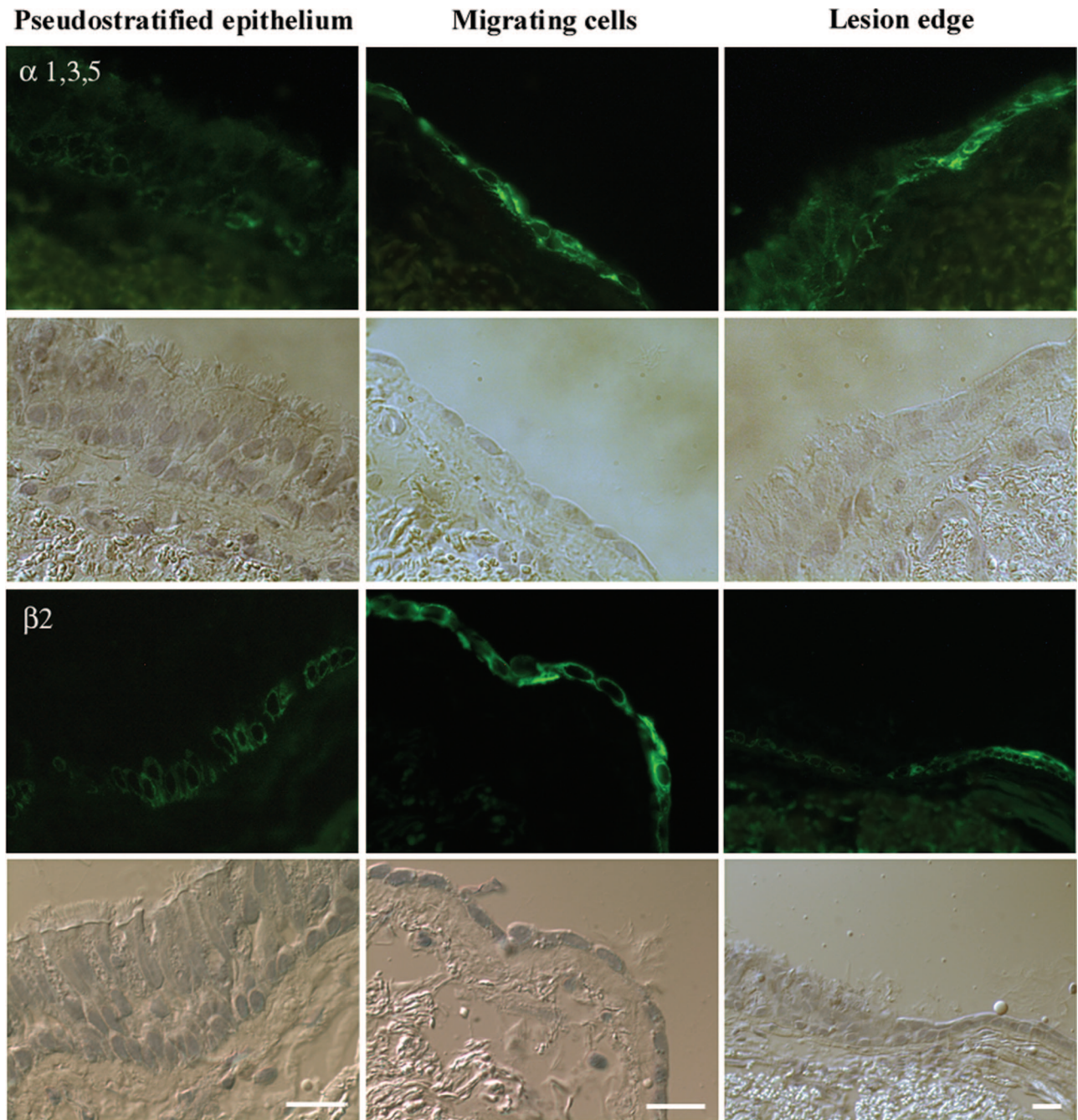


**Figure 1.** Identification of nicotinic receptors in repairing bronchial tissues. Normal human epithelium was locally wounded and maintained in culture for 1 day as described in Materials and Methods. The localization of nAChRs was studied by immunofluorescence using the rat mAb-210, specific for the  $\alpha 1$ ,  $\alpha 3$ , and  $\alpha 5$  subunits (**top**), or the rat mAb-290 monoclonal antibody, specific for the  $\beta 2$  subunit (**bottom**), with Alexa Fluor 488 conjugate (green color in dark panels). **Left column:** Stationary cells in the unwounded pseudostratified normal epithelium. **Middle column:** Migrating cells in the wounded area. **Right column:** Transition area between the normal unwounded epithelium and the migrating cells. Scale bars, 20  $\mu$ m.

## Results

### $\alpha 3\alpha 5\beta 2$ -nAChRs Are Overexpressed in Migrating HBECS

We studied the distribution of nAChRs in *ex vivo* epithelia undergoing repair. In normal pseudostratified epithelium located away from the wound, nAChRs could be detected with both the anti- $\alpha 1,3,5$  mAb-210 and the anti- $\beta 2$  mAb-290 antibody in the basal layer of the epithelium

(Figure 1). These basal cells were weakly labeled by the antibodies compared to epithelial cells migrating to cover the wounded area. Cells that were positive for  $\alpha 1,3,5$  and  $\beta 2$  subunits, both in the normal epithelium and in migrating cells, could be identified as basal cells as a result of their immunoreactivity for antibodies specific for cytokeratins 13 and 14 (data not shown). At the lesion edge, we observed the transition between the thick pseudostratified epithelium and the flat epithelial layer spreading over the denuded wounded surface. In this transition region,

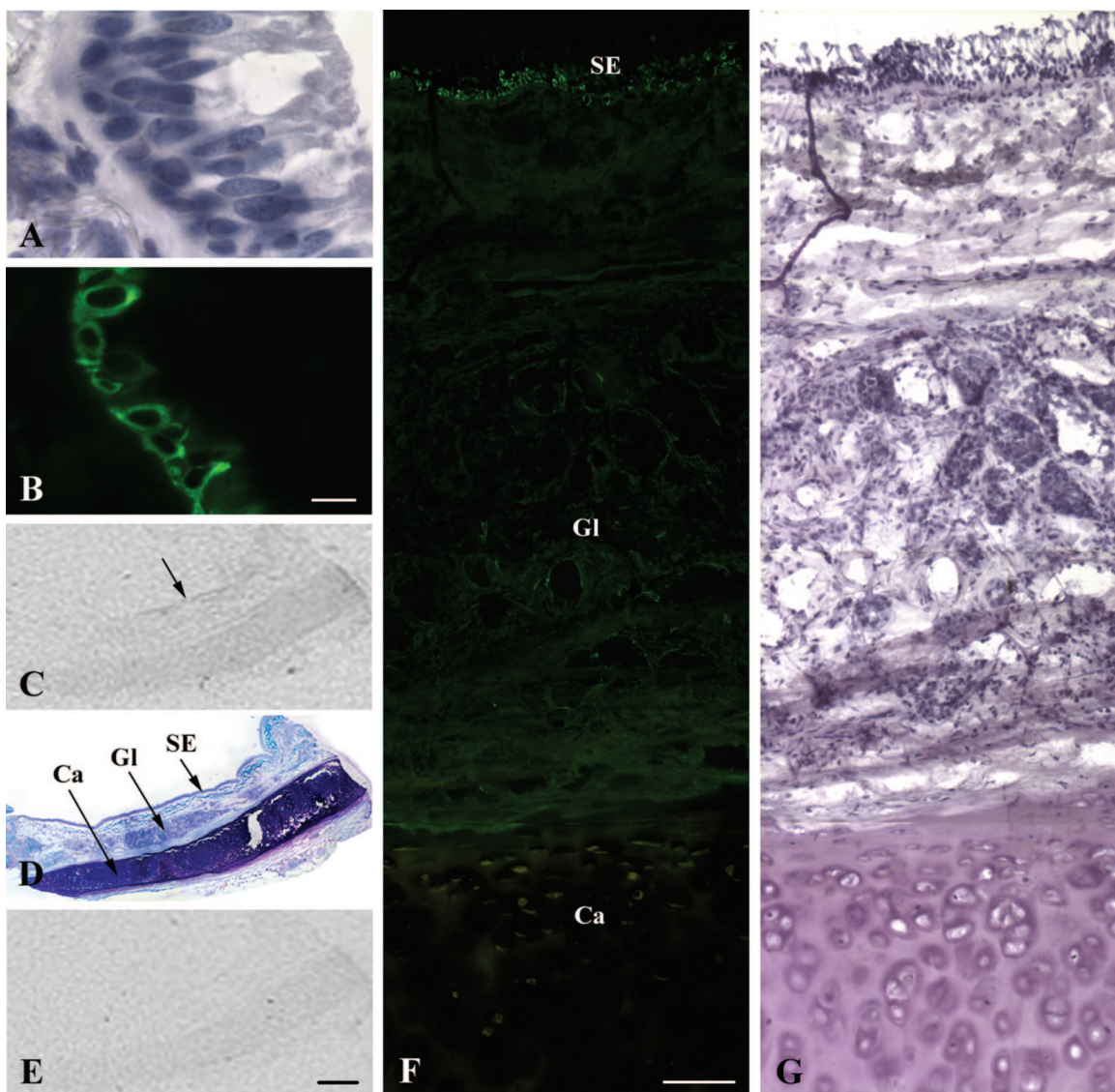


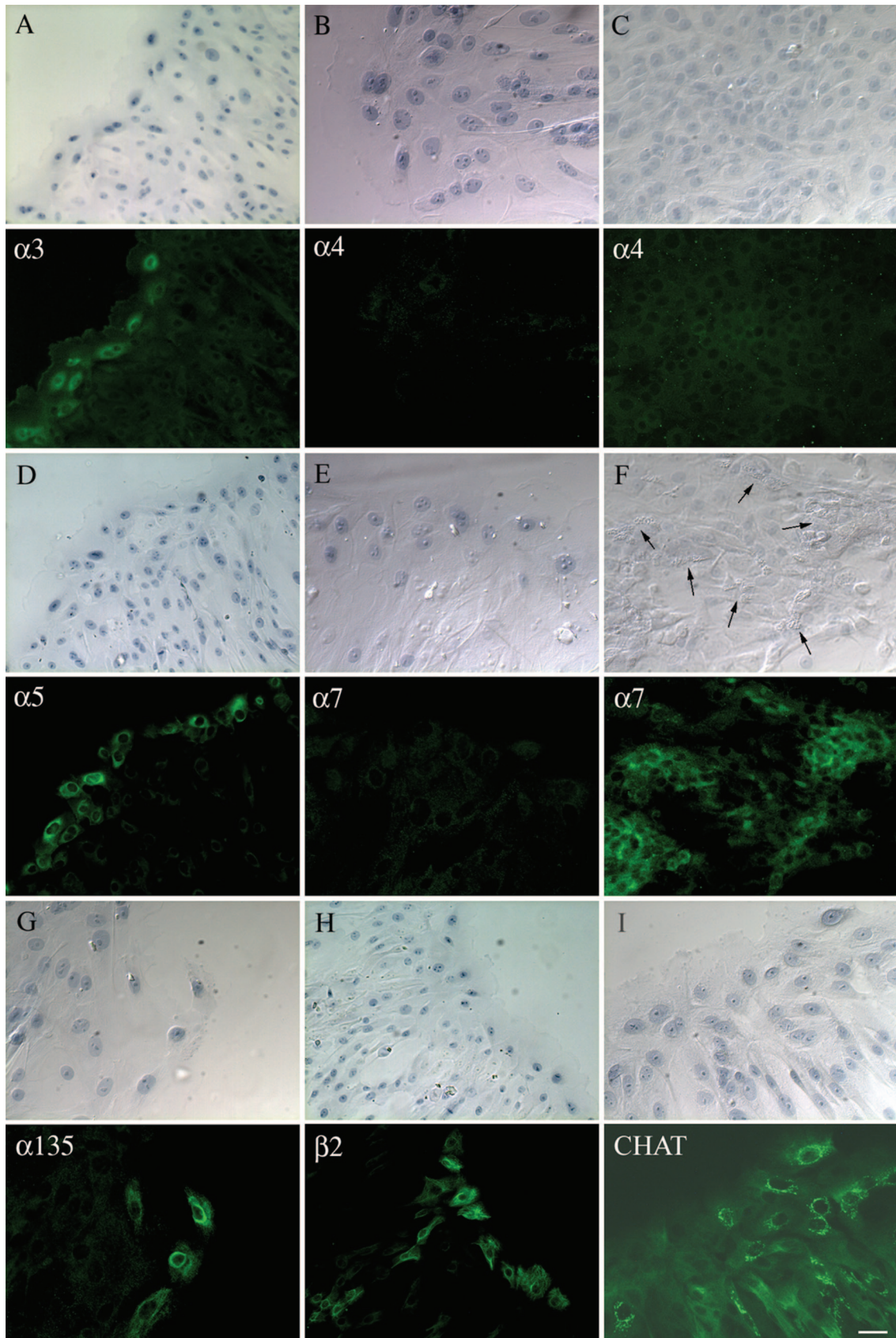
**Figure 2.** Localization of  $\beta 2$ -nAChRs and of binding sites for [ $^{125}$ I]-epibatidine in the bronchial epithelium. The localization of the  $\beta 2$  subunit of nAChRs was evaluated using an immunofluorescent labeling technique with the mAb-290 antibody in 5- $\mu$ m-thick (A and B) or 20- $\mu$ m-thick (F and G) sections of human bronchial tissues. Binding sites for epibatidine were identified in 20- $\mu$ m-thick sections in the absence (C) or presence (E) of 1 mmol/L nicotine, as described in Materials and Methods. C, E, and F correspond to serial 20- $\mu$ m sections of the same bronchial tissue. A, D, and G depict hematoxylin (A and G) or toluidine blue (D) staining of sections corresponding to immunofluorescence or autoradiography presented in B, C, and F, respectively. SE, surface epithelium; Gl, submucosal glands; Ca, cartilage. Scale bars: 10  $\mu$ m (A, B); 1 mm (C-E); or 100  $\mu$ m (F, G).

flat migrating basal cells were more intensely labeled for the presence of nAChRs than cuboidal basal cells in normal epithelium. High magnification of  $\beta 2$  subunit labeling revealed that  $\beta 2$  was distributed both in the cytoplasm and at the cell surface in basal cells, suggesting that the mAb-290 antibody recognized both immature cytoplasmic and mature membranous forms of  $\beta 2$ -nAChRs (Figure 2, A and B). Immunoreactivity for  $\beta 2$ -nAChRs was observed essentially in basal cells of the

surface bronchial epithelium, with some peripheral glandular cells in the submucosa also weakly labeled (Figure 2, F and G). Epibatidine is a potent nicotinic agonist with high affinity for human  $\alpha 3\beta 2$ - and  $\alpha 3\beta 4$ -nAChRs.<sup>32</sup> When used at a 200 pmol/L concentration, [ $^{125}$ I]-epibatidine binds to the cells present at the surface of bronchial epithelium (Figure 2C). The binding of epibatidine was abolished in the presence of 1 mmol/L nicotine (Figure 2E).

**Figure 3.** Identification of nAChRs and choline acetyltransferase in repairing HBEC cultures. One day after injuring primary cultures of HBECs, cultures were fixed and evaluated, using immunofluorescent labeling techniques with Alexa Fluor 488 conjugates, for the distribution of nAChR subunits with the following antibodies: C-18-Ab for  $\alpha 3$  subunit (A), mAb-8A4 for  $\alpha 4$  subunit (B and C), D-19-Ab for  $\alpha 5$  subunit (D), H-302-Ab for  $\alpha 7$  subunit (E and F), mAb-210 for  $\alpha 1,3,5$  subunits (G), mAb-290 for  $\beta 2$  subunit (H). The presence of choline acetyltransferase (CHAT) was also evaluated with the mAb-5270 (I). Micrographs correspond to the edge of the wounds (A, B, D, E, G-I) or to stationary cells in the unwounded area (C and F). Arrows in F point to ciliated cells. Scale bars: 50  $\mu$ m (A, D, H); 25  $\mu$ m (B, C, E-G, and I).





When primary and confluent cultures of HBECs were locally wounded, cells at the edge of the wound rapidly spread and migrated to cover the denuded area.<sup>1,26,30</sup> During the wound repair process, the  $\alpha 3$ ,  $\alpha 5$ , and  $\beta 2$  subunits of nAChRs were predominantly found in cells lining the wound edge and migrating onto the damaged area (Figure 3, A, D, G, and H). We could not detect the  $\alpha 4$  subunit in migrating cells or in confluent stationary cells (Figure 3, B and C). Subunit  $\alpha 7$  was not observed in migrating cells (Figure 3E) but was detected in areas of confluent and differentiated cells, as confirmed by the presence of ciliated cells (Figure 3F). Choline acetyltransferase, the enzyme that mediates ACh synthesis, was detected in the cytosol of both migrating and stationary cells (Figure 3I).

Because  $\alpha 3$ ,  $\alpha 5$ , and  $\beta 2$  subunits, along with  $\beta 4$  subunit, have been shown to be present in the same pentameric form of nAChR, at least in neurons,<sup>33</sup> we investigated the possible association between  $\alpha 3$ ,  $\alpha 5$ , and  $\beta 2$  in migrating HBECs. The co-assembly of  $\alpha 3$ ,  $\alpha 5$ , and  $\beta 2$  subunits was demonstrated by immunoprecipitating nAChRs from protein extracts of migrating HBECs with subunit-specific polyclonal antibodies (C18-Ab to  $\alpha 3$ , D19-Ab to  $\alpha 5$ , and C20-Ab to  $\beta 2$ ) and then detecting the precipitated subunits by Western blots using another set of subunit-specific monoclonal antibodies (mAb-210 to  $\alpha 1,3,5$ ; mAb-268 to  $\alpha 5$ ; and mAb-290 to  $\beta 2$ ). Each time we precipitated one of the three subunits ( $\alpha 3$ ,  $\alpha 5$ , or  $\beta 2$ ), we were able to detect the other two subunits on the immunoblots (Figure 4), suggesting that  $\alpha 3$ ,  $\alpha 5$ , and  $\beta 2$  subunits were co-assembled in the same nAChR, the  $\alpha 3\beta 2$ -nAChR, in migrating HBECs. The three subunits detected by immunoblot, had molecular masses (56 to 57 kD) that corresponded to the expected sizes deduced from their cDNA sequences (57.2 kD for  $\alpha 3$ , 56.3 kD for  $\alpha 5$ , and 56.9 kD for  $\beta 2$ ). Other proteins with molecular masses 60 to 70 kD were also detected on immunoblots even in the presence of a control precipitating antibody but were not detected in the absence of precipitating antibody, suggesting that these proteins nonspecifically bound IgG molecules during the immunoprecipitation. Immunoprecipitation with the D19 anti- $\alpha 5$  antibody resulted in a more intense band on the three immunoblots compared with the C18 and C20 antibodies, suggesting that  $\alpha 3\alpha 5\beta 2$ -nAChR immunoprecipitation was more efficiently achieved with the D19 antibody.

By using RT-PCR techniques, we confirmed the presence of transcripts for  $\alpha 3$ ,  $\alpha 5$ ,  $\alpha 7$ , and  $\beta 2$  subunits of nAChRs in migrating HBECs. The  $\beta 4$  subunit, for which we had no available antibody, could also be detected as mRNA transcript in migrating cells. The primers for the  $\alpha 3$ ,  $\alpha 5$ ,  $\alpha 7$ ,  $\beta 2$ , and  $\beta 4$  subunits yielded products of expected size whereas the  $\alpha 4$  primers did not yield PCR products (Figure 5).

### *The in Vitro Wound Repair of the Bronchial Epithelium Is Modulated by Agonists and Antagonists of $\alpha 3\alpha 5\beta 2$ -nAChRs*

Because  $\alpha 3\alpha 5\beta 2$ -nAChRs were more markedly identified in HBECs when they migrated to repair a wound in both *ex vivo* and *in vitro* models, we hypothesized that nAChRs

were involved in the wound repair process. We tested whether a modulation of nAChR activity, by agonists or antagonists, influenced the wound repair process. By using an *in vitro* model of bronchial epithelium wound repair, we quantified the speed of the wound closure in the presence of nAChR agonists (nicotine and ACh) or antagonists (mecamylamine, a noncompetitive reversible antagonist of  $\alpha/\beta$  heteromer nAChRs;  $\alpha$ -bungarotoxin, a highly selective antagonist of  $\alpha 7$ -nAChR;<sup>34</sup>  $\alpha$ -conotoxin MII, a highly selective antagonist of the  $\alpha 3\beta 2$ -nAChRs;<sup>35,36</sup> and  $\kappa$ -bungarotoxin, a selective and slowly reversible antagonist of  $\alpha 3\beta 2$  neuronal nAChRs<sup>37</sup>). After a 15 hour-exposure to 1 mmol/L nicotine or ACh, we observed a more rapid wound closure; however, the wound repair speed was reduced in the presence of 1 mmol/L mecamylamine or 1  $\mu$ mol/L  $\kappa$ -bungarotoxin (Figure 6, micrographs in A). The wound repair index increased in the presence of  $10^{-5}$  to  $10^{-3}$  mol/L nicotine ( $10^{-5}$  mol/L: +9.6%,  $P = 0.0389$ ;  $10^{-4}$  mol/L: +18%,  $P = 0.0201$ ;  $10^{-3}$  mol/L: +25.2%,  $P = 0.0201$ ) or ACh ( $10^{-5}$  mol/L: +14.6%,  $P = 0.0201$ ;  $10^{-4}$  mol/L: +23.6%,  $P = 0.0201$ ;  $10^{-3}$  mol/L: +34.6%,  $P = 0.0201$ ). The wound repair index was decreased in the presence of  $10^{-5}$  to  $10^{-3}$  mol/L mecamylamine ( $10^{-5}$  mol/L: -18%,  $P = 0.0201$ ;  $10^{-4}$  mol/L: -46%,  $P = 0.0201$ ;  $10^{-3}$  mol/L: -76%,  $P = 0.0201$ ), in the presence of 1 or 10  $\mu$ mol/L  $\alpha$ -conotoxin MII (-17%,  $P = 0.0201$ ; -49%,  $P = 0.0201$ ; respectively) and in the presence of 0.1 or 1  $\mu$ mol/L  $\kappa$ -bungarotoxin (-38%,  $P = 0.0201$ ; -73%,  $P = 0.0201$ , respectively) (Figure 6B). Because  $\kappa$ -bungarotoxin more efficiently inhibited  $\alpha 3\alpha 5\beta 2$ -nAChR-mediated wound repair than  $\alpha$ -conotoxin MII,  $\kappa$ -bungarotoxin was preferred to  $\alpha$ -conotoxin MII in the following experiments.

### *Antagonists of $\alpha 3\alpha 5\beta 2$ -nAChRs Decrease the in Vitro Migration of HBECs*

We quantified and studied cell migration speeds at the edge of the wound and investigated the effect of mecamylamine,  $\alpha$ -bungarotoxin, and  $\kappa$ -bungarotoxin. After exposure of cells to mecamylamine, the cell migration speed at the edge of the wound progressively declined (Figure 7A), the effect of mecamylamine being dose- and time-dependent (Figure 7B). After a 1-hour exposure to 1 mmol/L mecamylamine, we observed a 55% decrease in the cell migration speed. The effect of mecamylamine was reversible as cells rapidly returned to a normal migration speed after mecamylamine was removed from the culture medium (Figure 7C). In the presence of 1  $\mu$ mol/L  $\kappa$ -bungarotoxin, the migration speed of the cells also progressively declined, with a 45% decrease in cell migration speed after a 1-hour exposure to  $\kappa$ -bungarotoxin. Exposure of migrating HBECs to 10  $\mu$ mol/L  $\alpha$ -bungarotoxin had no significant effect on cell migration throughout a 1-hour incubation period (Figure 7D).



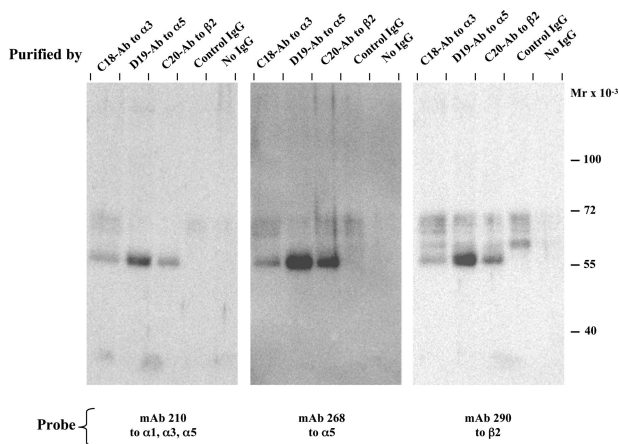


**Figure 4.** Immunoblot analysis showing that  $\beta 2$  associates with  $\alpha 3$  and  $\alpha 5$  subunits of nAChRs in migrating HBECs. Nicotinic receptors were solubilized in RIPA buffer from migrating HBECs in culture and immunopurified from cell extracts with the following antibodies: goat C-18-Ab for  $\alpha 3$  subunit, goat D-19-Ab for  $\alpha 5$  subunit, goat C-20-Ab for  $\beta 2$  subunit, control goat IgG, or in absence of antibody (no IgG). Samples were analyzed by immunoblot technique for their reactivity with the following rat monoclonal antibodies: mAb-210 for  $\alpha 1,3,5$  subunits, mAb-268 for  $\alpha 5$  subunit, and mAb-290 for  $\beta 2$  subunit, as described in Materials and Methods. Molecular weights of standard proteins (Bio-Rad) have been reported on the **right**.

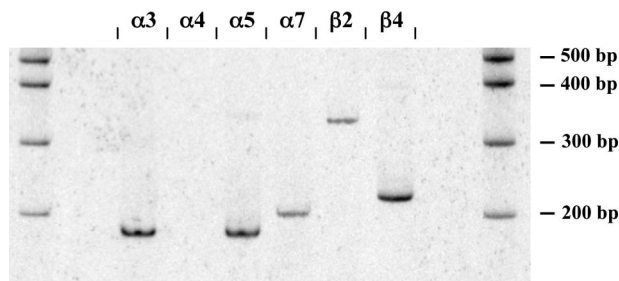


**Figure 5.** Detection of  $\alpha 3$ ,  $\alpha 5$ ,  $\alpha 7$ ,  $\beta 2$ , and  $\beta 4$  subunit transcripts of nAChRs in cultured HBECs by RT-PCR. RT-PCR experiments were performed using RNA extracted from migrating HBECs in culture and primers specific for the different neuronal nAChR subunits, as indicated. The positions of a 100-bp ladder are reported on the **right**.

### $\alpha 3\alpha 5\beta 2$ -nAChRs Modulate Intracellular Calcium in Migrating HBECs

Nicotinic receptors belong to the family of ligand-gated multisubunit ion channels, activation of which mediates the entrance of monovalent or divalent cations into the cell. Because  $\text{Ca}^{2+}$  plays a crucial role in regulating many functions in HBECs<sup>38</sup> and is involved in the regulation of cell migration,<sup>39,40</sup> we studied the variations in  $[\text{Ca}^{2+}]_i$  in migrating HBECs on exposure to nicotine. The addition of 1 mmol/L nicotine to the medium of HBEC cultures undergoing wound repair rapidly increased  $[\text{Ca}^{2+}]_i$  in migrating cells (Figure 8). The amplitude of  $[\text{Ca}^{2+}]_i$  increase was more pronounced in the cells lining the wound edge (zone 1 in Figure 8A), with  $[\text{Ca}^{2+}]_i$  rising from 50 nmol/L to 170 nmol/L. In cells located away from the wound edge,  $[\text{Ca}^{2+}]_i$  did not rise greater than 70 nmol/L after the addition of nicotine (Figure 8B). The increase in  $[\text{Ca}^{2+}]_i$  was transient because it lasted  $\sim 1$  minute (Figure 8, B and C). The effect of nicotine on  $[\text{Ca}^{2+}]_i$  was dose-dependent because 0.5 and 1 mmol/L concentrations of nicotine elicited a progressive

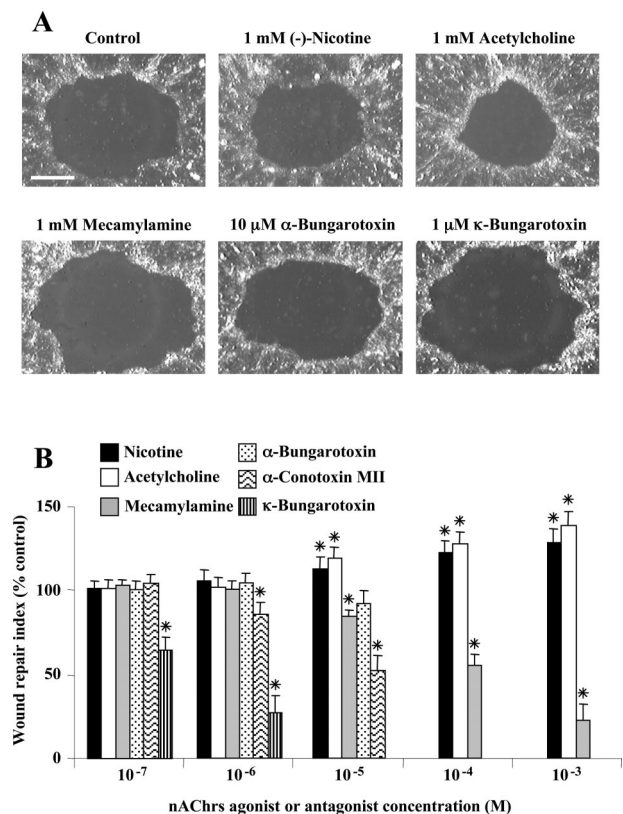


**Figure 6.** Effect of nicotinic agonists and antagonists on the wound repair of HBECs in culture. Immediately after wounding, primary HBEC cultures were exposed for 15 hours to different concentrations ( $10^{-7}$  to  $10^{-3}$  mol/L) of nicotinic receptor agonists (nicotine and ACh) or antagonists (mecamylamine,  $\alpha$ -bungarotoxin,  $\alpha$ -conotoxin MII, and  $\kappa$ -bungarotoxin). The wound repair index was then calculated for each condition, as described in Materials and Methods. **A:** Phase contrast micrographs of repairing cultures at the end of the experiment in the control condition or in the presence of 1 mmol/L nicotine, 1 mmol/L ACh, 1 mmol/L mecamylamine, 10  $\mu$ mol/L  $\alpha$ -bungarotoxin, or 1  $\mu$ mol/L  $\kappa$ -bungarotoxin. **B:** During the wound repair process, the wound repair index was evaluated in each condition and compared (Mann-Whitney test) to the same parameter in the control experiment:  $*P < 0.05$ . Each condition (mean  $\pm$  SD) was run in triplicates. Scale bar, 1 mm.

increase in  $[\text{Ca}^{2+}]_i$  (+158%,  $P = 0.02$  and + 281%,  $P = 0.02$ , respectively) (Figure 9, A–D). We did not observe any significant variations in  $[\text{Ca}^{2+}]_i$  on exposure with nicotine concentrations lower than 0.5 mmol/L. The effect of nicotine on  $[\text{Ca}^{2+}]_i$  could be prevented by preincubating cells with 1 mmol/L mecamylamine (Figure 9E). The effect of mecamylamine was reversible because the nicotine-induced increase in  $[\text{Ca}^{2+}]_i$  in migrating cells could be partially restored after removing mecamylamine from the culture medium (Figure 10). The nicotine-induced increase of  $[\text{Ca}^{2+}]_i$  in migrating cells was completely abolished in the presence of 1 mmol/L mecamylamine (Figures 9E and 10) but did not significantly change after a 60-minute exposure to 1 or 10  $\mu$ mol/L  $\alpha$ -bungarotoxin (Figure 9, F and G). On the contrary,  $\kappa$ -bungarotoxin prevented 88% of the nicotine-induced increase of  $[\text{Ca}^{2+}]_i$  in migrating cells at a 1  $\mu$ mol/L concentration (Figure 9I).

### Discussion

Our results suggest that  $\alpha 3\alpha 5\beta 2$ -nAChRs contribute to the wound repair of the human bronchial epithelium

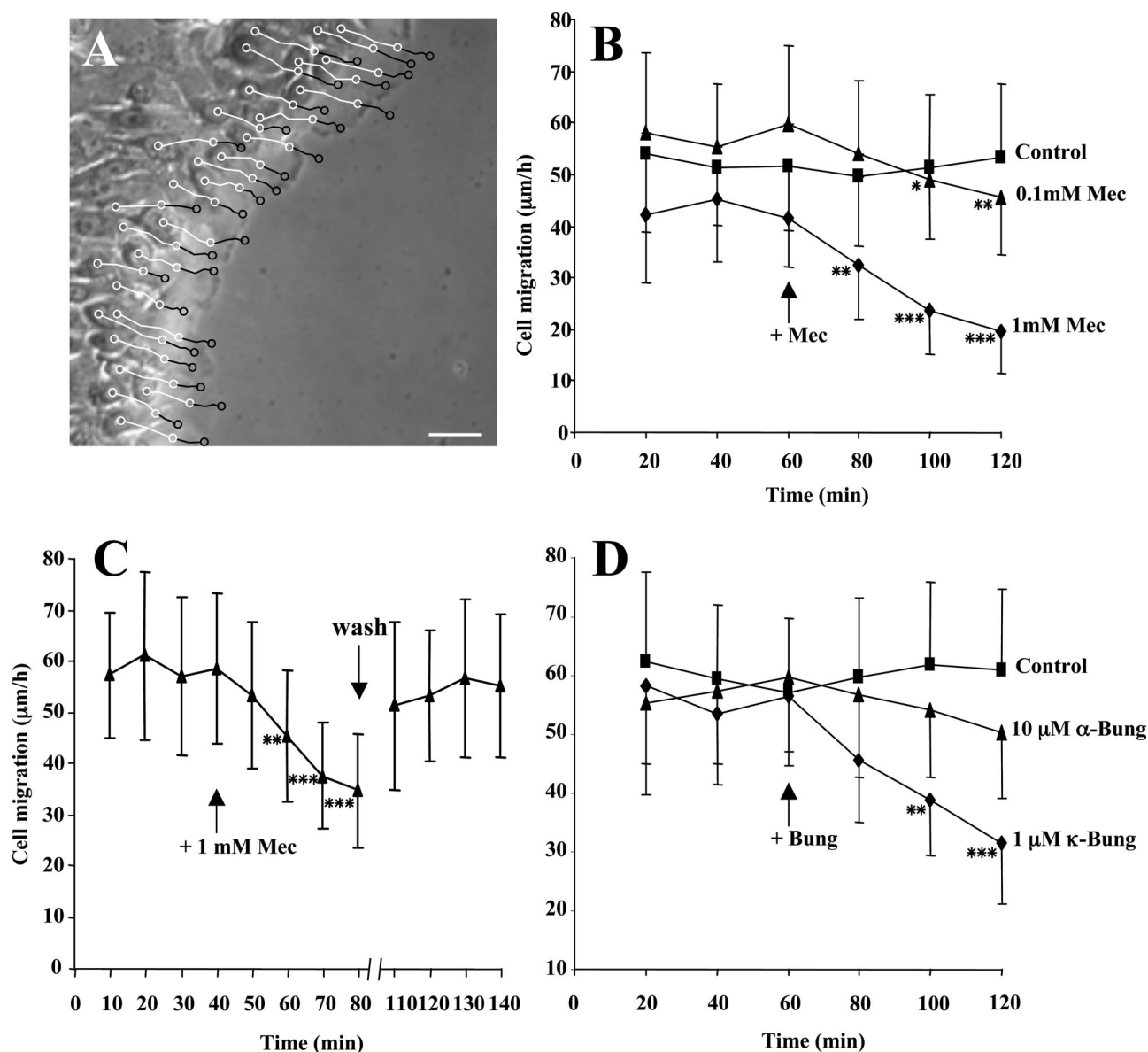


**Figure 7.** Effect of mecamlamine, α-bungarotoxin, and κ-bungarotoxin on HBEC migration. One day after injury of primary cultures of HBECs, cell migration was measured as described in Materials and Methods. **A:** Phase contrast micrograph of migrating HBECs at the beginning of the experiment and trajectories of individual cells during the control period (in white) and in the presence of 1 mmol/L mecamlamine (in black), corresponding to the values reported in **B** (1 mmol/L Mec). Migration speeds of the cells ( $n = 30$ ) located at the edge of the wound were determined every 20 minutes (**B** and **D**) or 10 minutes (**C**) throughout a 60-minute (**B** and **D**) or 40-minute (**C**) control period. **B:** At 60 minutes, 0.1 mmol/L (filled triangles) or 1 mmol/L (filled diamonds) mecamlamine (+Mec) or its vehicle (culture medium, filled squares) was added to the culture medium, and the migration speeds of the same cells were monitored throughout an additional 60-minute period. **C:** At 40 minutes, 1 mmol/L mecamlamine (+1 mM Mec) was added to the culture medium, and the migration speeds of the same cells were monitored throughout an additional 40-minute period. At 80 minutes (wash), mecamlamine was removed, cells were washed with fresh culture medium and the migration speeds of the same cells were monitored again throughout an additional 40-minute period. **D:** At 60 minutes, 10 μmol/L α-bungarotoxin (filled triangles) or 1 μmol/L κ-bungarotoxin (filled diamonds) (+Bung) or their vehicle (culture medium, filled squares) were added to the culture medium, and the migration speeds of the same cells were monitored throughout an additional 60-minute period. Each bar represents the mean  $\pm$  SD of the migration speed of 30 cells. Cell migration at each time and in the presence of mecamlamine, α-bungarotoxin, or κ-bungarotoxin was compared (paired *t*-test) to cell migration during the control period: \* $P < 0.05$ , \*\* $P < 0.01$ , \*\*\* $P < 0.001$ . Scale bar, 40 μm.

based on the following data. First, the expression of α3, α5, and β2 subunits of nAChRs is up-regulated in migrating cells in both *ex vivo* and *in vitro* models of human bronchial epithelium injury and repair. Second, the nicotinic agonists nicotine and ACh accelerate the wound repair process. Third, mecamlamine, a preferential antagonist of α/β heteromer nAChRs, and selective antagonists of α3/β2 neuronal nAChRs, α-conotoxin MII, and κ-bungarotoxin, delay the wound repair process. Addi-

tionally, κ-bungarotoxin decreases the migration speed of *in vitro* repairing epithelial cells, whereas α-bungarotoxin, an α7-nAChR antagonist, has only a minor effect on the *in vitro* cell migration and wound repair process. Fourth, exposure of repairing HBEC cultures to nicotine results in a transient increase in intracellular calcium in elongated migrating cells that are located close to the edge of the wound. Finally, the nicotine-induced increase in  $[Ca^{2+}]_i$  in migrating cells is blocked by mecamlamine



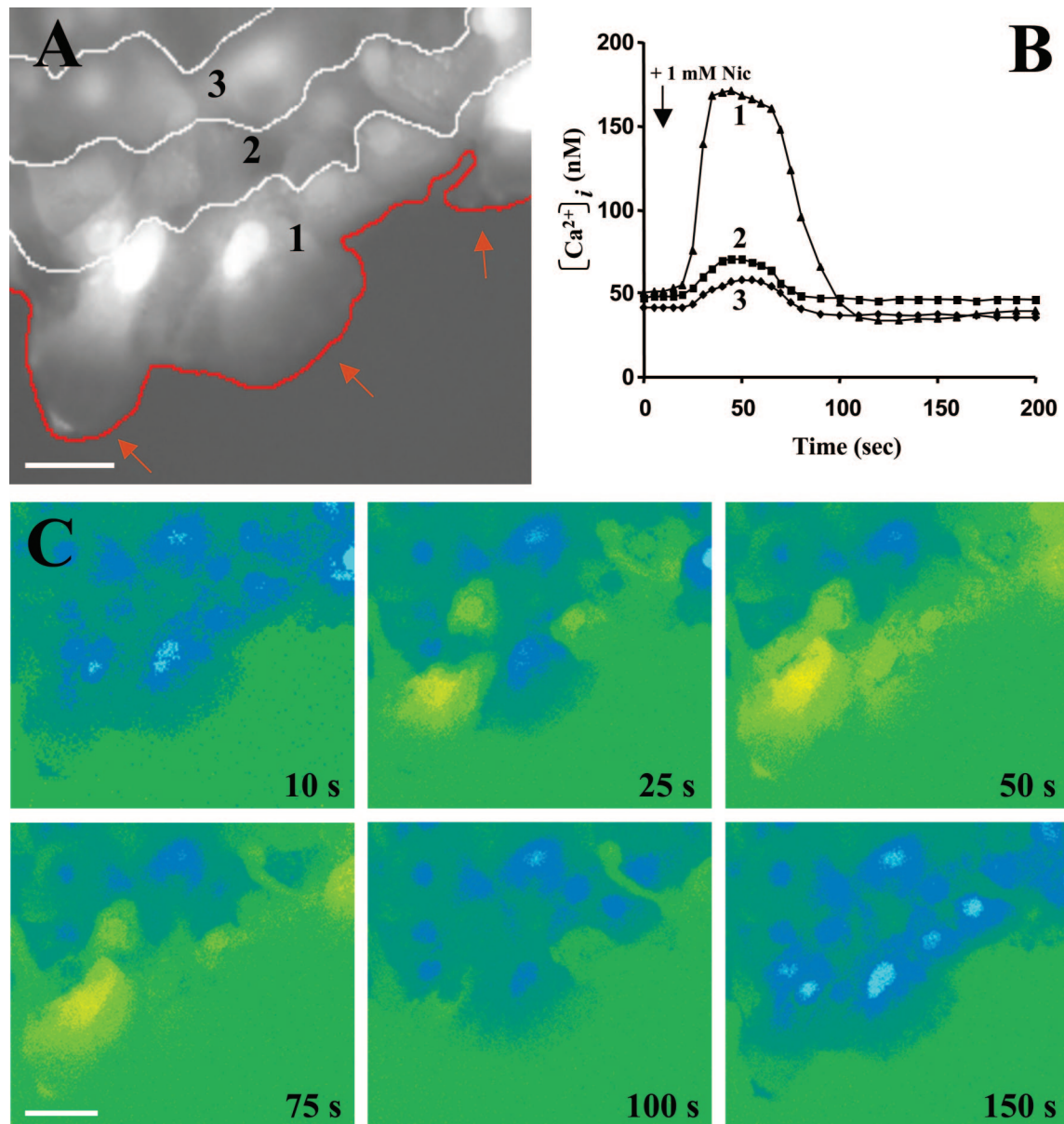


**Figure 8.** Nicotine increases the  $[Ca^{2+}]_i$  in migrating HBECs in culture. One day after injuring primary cultures of HBECs, cells were loaded with  $3 \mu\text{mol/L}$  Fura-2 for the measurement of  $[Ca^{2+}]_i$  as described in Materials and Methods. The  $[Ca^{2+}]_i$  was recorded every 10 seconds throughout a 200-second period in three different zones as reported in **A**. Zone 1 corresponds to cells lining the wound edge; zones 2 and 3 correspond to the second and third lines of cells from the wound edge, respectively. The **red line** in **A** corresponds to the forefront of the cellular protrusions lining the wound edge. **Arrows** point at lamellipodia of three advancing cells. **B**: Evolution of  $[Ca^{2+}]_i$  in zones 1, 2, and 3. Nicotine ( $1 \text{ mmol/L}$ ) was added to the culture medium 20 seconds after the beginning of  $[Ca^{2+}]_i$  recording. **C**: Pseudocolor calcium ratio ( $340/380 \text{ nm}$ ; blue, low  $[Ca^{2+}]_i$ ; yellow, high  $[Ca^{2+}]_i$ ), images were taken at 10, 25, 50, 75, 100, and 150 seconds after addition of  $1 \text{ mmol/L}$  nicotine. Scale bars,  $20 \mu\text{m}$ .

and  $\kappa$ -bungarotoxin but unchanged in the presence of  $\alpha$ -bungarotoxin.

Our results demonstrate that the  $\alpha 3\alpha 5\beta 2$ -nAChR is involved in bronchial epithelium wound repair, whereas the  $\alpha 7$ -nAChR does not seem to play any crucial role in this process. The specific antagonist of the  $\alpha 7$ -nAChR,  $\alpha$ -bungarotoxin, did not induce a significant decrease in the wound repair index, even when tested at a  $10 \mu\text{mol/L}$  concentration. Contrary to the  $\alpha 3\alpha 5\beta 2$ -nAChR, the  $\alpha 7$ -nAChR was not identified in migratory HBECs but, rather, was concentrated on the lateral cell border of confluent cells located away from the wound edge. These highly

packed cells were shown to be differentiated, as confirmed by the presence of numerous ciliated cells. On the other hand, wound-repairing migrating HBECs are characterized by a dedifferentiated phenotype<sup>1</sup> with some mesenchymal properties.<sup>29</sup> The  $\alpha 7$ -nAChR plays a central role in the late stages of keratinocyte differentiation in the epidermis by regulating expression of the cell-cycle progression, apoptosis, and terminal differentiation genes.<sup>41</sup> In cultured keratinocytes,  $\alpha 7$ -immunoreactive cells are large immotile cells in contrast to the small highly mobile cells immunostained with the  $\alpha 3$ ,  $\alpha 5$ , and  $\beta 2$  antibodies.<sup>42</sup> From these observations, we conclude

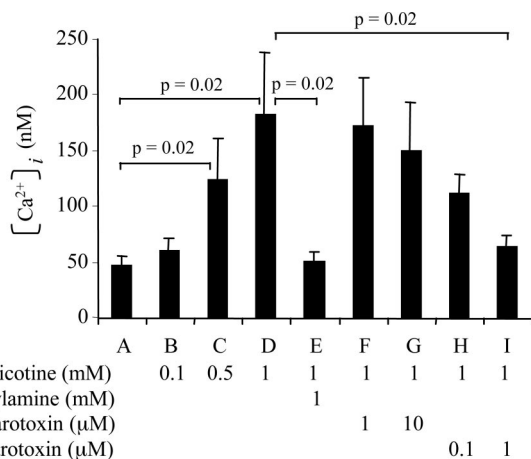


**Figure 9.** Effects of nicotine, mecamylamine,  $\alpha$ -bungarotoxin, and  $\kappa$ -bungarotoxin on the  $[Ca^{2+}]_i$  in migrating HBECs. The effects of nicotine and the nicotinic receptor antagonists mecamylamine,  $\alpha$ -bungarotoxin, and  $\kappa$ -bungarotoxin on the  $[Ca^{2+}]_i$  were studied by image analysis in migrating HBECs located at the wound edge on day 1 of the wound repair process, as described in Materials and Methods.  $[Ca^{2+}]_i$  was monitored in the absence (A) or in the presence of 0.1 mmol/L (B), 0.5 mmol/L (C), or 1 mmol/L (D) nicotine. After a 5-minute incubation with 1 mmol/L mecamylamine (E), with 0.1  $\mu$ mol/L (H) or 1  $\mu$ mol/L (I)  $\kappa$ -bungarotoxin, or after a 60-minute incubation with 1  $\mu$ mol/L (F) or 10  $\mu$ mol/L (G)  $\alpha$ -bungarotoxin, cells were challenged with 1 mmol/L nicotine during the  $[Ca^{2+}]_i$  recording. Results are expressed as mean  $[Ca^{2+}]_i \pm$  SD for four different experiments conducted on primary cultures of HBECs derived from four different bronchial samples. The significance of the differences between groups was determined using Mann-Whitney test.

that the  $\alpha 3\alpha 5\beta 2$ -nAChR and  $\alpha 7$ -nAChR may be involved in HBEC migration and differentiation, respectively. Recently, Chernyavsky and colleagues<sup>23</sup> have observed that the  $\alpha 3\beta 2$ -nAChR regulates *in vitro* the keratinocyte random migration, whereas the  $\alpha 7$ -nAChR is rather involved in the directional migration of keratinocytes against a gradient of nicotinic agonists. Similarly,  $\alpha 7$ -nAChR mediates migration of vascular smooth muscle

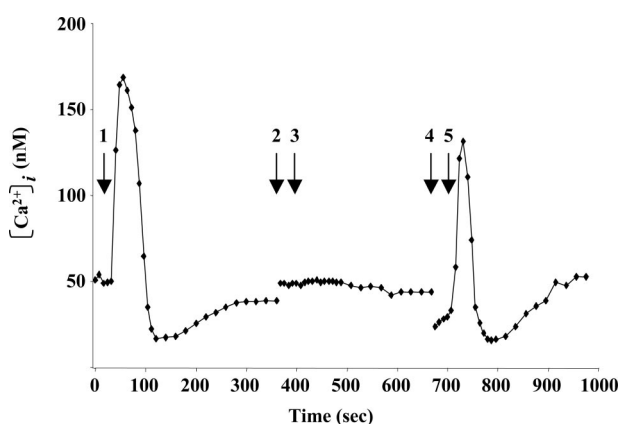


**Figure 10.** Mecamylamine reversibly inhibits nicotine-induced  $[Ca^{2+}]_i$  increase in migrating HBECs in culture. The variation of nicotine-induced  $[Ca^{2+}]_i$  in migrating HBECs, located at the wound edge on day 1 of the wound repair process, was followed as described in Figure 8. 1, Nicotine (1 mmol/L) was added to the culture medium and  $[Ca^{2+}]_i$  was monitored for 340 seconds. 2, Culture medium was removed, cells were washed, and 1 mmol/L mecamylamine was added in the culture medium. 3, Nicotine (1 mmol/L) was added to the culture medium, and  $[Ca^{2+}]_i$  was monitored for an additional 260-second period. 4, Cells were washed with the culture medium. 5, Nicotine (1 mmol/L) was added to the culture medium and  $[Ca^{2+}]_i$  was monitored for an additional 260-second period. Throughout the entire experiment,  $[Ca^{2+}]_i$  was monitored in the same group of migrating HBECs.

cells toward nicotine.<sup>15</sup> In these experiments, cells were induced to migrate according to a centrifugal random or directional movement. In our *ex vivo* and *in vitro* models of HBEC migration, bronchial tissues or confluent HBEC cultures were locally injured. This injury resulted in local cell desquamation similar to that observed *in vivo* in remodeled bronchial epithelia,<sup>43–45</sup> and the wound repair process was characterized by a uniform centripetal direction of cell movement.<sup>46</sup> In centrifugal models of cell migration, we observed that many cells migrated as individual cells and had random trajectories (unpublished observations), whereas in centripetal models all cells had a coordinated movement.<sup>1,46</sup> We performed all of the experiments described here by using freshly isolated HBECs and short-term exposures to nicotinic agonists. Our *in vitro* results are thus likely to be more relevant to an *in vivo* situation. In most other reports dealing with nAChR and cell migration, cells were chronically exposed to nicotinic agonists for up to 10 days before measurements of cell migration.<sup>19,23</sup> Long-term exposure to nicotine induces nAChR expression.<sup>12,47,48</sup> These differences both in migration models, centrifugal versus centripetal cell migration, in duration of agonist exposure and in tissue origin may explain the differences observed in the contribution of nAChRs in the migration of keratinocytes and bronchial epithelial cells.

We observed that the  $\alpha 3\alpha 5\beta 2$ -nAChR was identified, with a low level of expression compared with migrating HBECs, in the basal layer of the pseudostratified normal and stationary bronchial epithelium. The presence of  $\alpha 3\alpha 5\beta 2$ -nAChRs in the surface bronchial epithelium was confirmed by autoradiographic studies showing that [<sup>125</sup>I]-epibatidine, a potent nicotinic agonist with high affinity for human  $\alpha 3\beta 2$ - and  $\alpha 3\beta 4$ -nAChRs,<sup>32</sup> bound specifically to the cells present at the surface of bronchial epithelium. Similarly, keratinocytes present in the lower layers of the epidermis express  $\alpha 3\beta 2$ -nAChRs, which are suggested to be involved in maintaining the flat shape of the cells necessary to form a continuous layer over the epidermal basement membrane.<sup>12,19</sup> Because of continuous exposure to noxious inhaled agents, the airway epithelium is permanently injured and there is a continual shedding of surface epithelial cells; this requires a regenerative process that includes differentiation and proliferation.<sup>49</sup> The basal cells represent the major dynamic source of epithelial cells in the airway.<sup>50</sup> Differentiation of mature ciliated and secretory cells from basal cells requires changes in cell shape, elongation of the cells up to the airway lumen, and modifications of cell-cell and cell-extracellular matrix contacts, as in migrating repair cells. Moreover, cells that migrate to repair a wound retain some characteristics of basal cells and express cytokeratins 13 and 14.<sup>26,29</sup> Although this must be confirmed in future investigations, we can hypothesize that  $\alpha 3\alpha 5\beta 2$ -nAChRs involved in cell migration during wound repair may also have a role in the continuous renewal of bronchial epithelial cells.

We observed that exposure of migrating cells to nicotine induced a transient increase of intracellular calcium in cells lining the wound edge. We demonstrated the major contribution of the  $\alpha 3\alpha 5\beta 2$ -nAChR in the nicotine-



induced variations of intracellular calcium in migrating HBECs. nAChRs are ligand-gated channels selective for cations.<sup>51</sup> Because of the major role of intracellular calcium, many studies have focused on the  $\text{Ca}^{2+}$  permeability of nAChRs. The  $\alpha 7$ -nAChR has garnered much attention because it is highly permeable to  $\text{Ca}^{2+}$ <sup>52,53</sup> and thus regulates many  $\text{Ca}^{2+}$ -dependent cellular processes, such as cell plasticity, growth, migration, and survival.<sup>51</sup> The  $\alpha 3$ -nAChR was initially shown to have significant  $\text{Ca}^{2+}$  permeability, but much lower than that of the  $\alpha 7$ -nAChR.<sup>54,55</sup> The introduction of  $\alpha 5$  subunit in the  $\alpha 3\beta 2$ -nAChRs further increases  $\text{Ca}^{2+}$  permeability to values comparable to the  $\alpha 7$ -nAChR.<sup>56</sup> Because of the much slower desensitization rates of  $\alpha 3\beta 2$ -nAChRs compared with the  $\alpha 7$ -nAChR,<sup>33,57</sup>  $\alpha 3\alpha 5\beta 2$ -nAChRs could potentially, throughout prolonged periods, conduct more  $\text{Ca}^{2+}$  than could  $\alpha 7$ -nAChRs. This suggests that  $\alpha 3\alpha 5\beta 2$ -nAChRs may play more important roles than previously suspected in ACh-induced  $\text{Ca}^{2+}$ -mediated effects in nonneuronal cells. Influx of  $\text{Ca}^{2+}$  into the cell is determinant on the induction of locomotion, control of direction of locomotion, and modulation of shape of epithelial cells.<sup>39,58</sup> For example, intracellular  $\text{Ca}^{2+}$  concentrations correlate with leukocyte migration speed.<sup>39</sup> Our results showed that nicotine increased  $[\text{Ca}^{2+}]_i$  in migrating HBECs located close to the edge of the wound. We previously observed that these cells migrated to the wounded area with the highest velocity, compared to cells located away from the wound edge.<sup>30</sup> Our results thus demonstrate that cells at the wound edge migrate with a high velocity, have an overexpression of  $\alpha 3\alpha 5\beta 2$ -nAChRs and display a high  $\alpha 3\alpha 5\beta 2$ -nAChR-dependent increase in  $[\text{Ca}^{2+}]_i$  when exposed to nicotine, suggesting that  $\alpha 3\alpha 5\beta 2$ -nAChRs control HBEC migration by modulating  $[\text{Ca}^{2+}]_i$ .  $\alpha 3\alpha 5\beta 2$ -nAChRs in migrating cells are likely to be stimulated by ACh produced by migrating and stationary HBECs. Indeed, we observed that all HBECs in culture contained choline acetyltransferase, which mediates ACh synthesis.

In conclusion, we have observed that the  $\alpha 3\alpha 5\beta 2$ -nAChR modulates intracellular calcium in migrating HBECs and is involved in HBEC migration and wound repair of the bronchial epithelium. Cell migration is also a determinant during fetal development and invasion of cancer cells. The role of the  $\alpha 3\alpha 5\beta 2$ -nAChR in the establishment of the bronchial epithelium and the development of bronchial invasive cancers remains to be defined.

## References

- Zahm JM, Chevillard M, Puchelle E: Wound repair of human surface respiratory epithelium. *Am J Respir Cell Mol Biol* 1991, 5:242–248
- Shimizu T, Nishihara M, Kawaguchi S, Sakakura Y: Expression of phenotypic markers during regeneration of rat tracheal epithelium following mechanical injury. *Am J Respir Cell Mol Biol* 1994, 11:85–94
- Herard AL, Zahm JM, Pierrot D, Hinnrasky J, Fuchey C, Puchelle E: Epithelial barrier integrity during in vitro wound repair of the airway epithelium. *Am J Respir Cell Mol Biol* 1996, 15:624–632
- Galzi JL, Changeux JP: Neuronal nicotinic receptors: molecular organization and regulations. *Neuropharmacology* 1995, 34:563–582
- Zia S, Ndoye A, Nguyen VT, Grando SA: Nicotine enhances expression of the alpha 3, alpha 4, alpha 5, and alpha 7 nicotinic receptors modulating calcium metabolism and regulating adhesion and motility of respiratory epithelial cells. *Res Commun Mol Pathol Pharmacol* 1997, 97:243–262
- Maus AD, Pereira EF, Karachunski PI, Horton RM, Navaneetham D, Macklin K, Cortes WS, Albuquerque EX, Conti-Fine BM: Human and rodent bronchial epithelial cells express functional nicotinic acetylcholine receptors. *Mol Pharmacol* 1998, 54:779–788
- Wang Y, Pereira EF, Maus AD, Ostlie NS, Navaneetham D, Lei S, Albuquerque EX, Conti-Fine BM: Human bronchial epithelial and endothelial cells express alpha7 nicotinic acetylcholine receptors. *Mol Pharmacol* 2001, 60:1201–1209
- Proskocil BJ, Sekhon HS, Jia Y, Savchenko V, Blakely RD, Lindstrom J, Spindel ER: Acetylcholine is an autocrine or paracrine hormone synthesized and secreted by airway bronchial epithelial cells. *Endocrinology* 2004, 145:2498–2506
- Klapproth H, Reinheimer T, Metzen J, Munch M, Bittinger F, Kirkpatrick CJ, Hohle KD, Schemann M, Racke K, Wessler I: Non-neuronal acetylcholine, a signalling molecule synthesized by surface cells of rat and man. *Naunyn Schmiedeberg's Arch Pharmacol* 1997, 355:515–523
- Wessler I, Kirkpatrick CJ, Racke K: The cholinergic 'pitfall': acetylcholine, a universal cell molecule in biological systems, including humans. *Clin Exp Pharmacol Physiol* 1999, 26:198–205
- Erickson JD, Varoqui H, Schafer MK, Modi W, Diebler MF, Weihe E, Rand J, Eiden LE, Bonner TI, Usdin TB: Functional identification of a vesicular acetylcholine transporter and its expression from a "cholinergic" gene locus. *J Biol Chem* 1994, 269:21929–21932
- Grando SA, Horton RM, Pereira EF, Diethelm-Okita BM, George PM, Albuquerque EX, Conti-Fine BM: A nicotinic acetylcholine receptor regulating cell adhesion and motility is expressed in human keratinocytes. *J Invest Dermatol* 1995, 105:774–781
- Nguyen VT, Arredondo J, Chernyavsky AI, Kitajima Y, Grando SA: Keratinocyte acetylcholine receptors regulate cell adhesion. *Life Sci* 2003, 72:2081–2085
- Totti III N, McCusker KT, Campbell EJ, Griffin GL, Senior RM: Nicotine is chemotactic for neutrophils and enhances neutrophil responsiveness to chemotactic peptides. *Science* 1984, 223:169–171
- Li S, Zhao T, Xin H, Ye LH, Zhang X, Tanaka H, Nakamura A, Kohama K: Nicotinic acetylcholine receptor alpha7 subunit mediates migration of vascular smooth muscle cells toward nicotine. *J Pharmacol Sci* 2004, 94:334–338
- Dwivedi C, Long NJ: Effect of cholinergic agents on human spermatozoa motility. *Biochem Med Metab Biol* 1989, 42:66–70
- Zheng JQ, Felder M, Connor JA, Poo MM: Turning of nerve growth cones induced by neurotransmitters. *Nature* 1994, 368:140–144
- Owen A, Bird M: Acetylcholine as a regulator of neurite outgrowth and motility in cultured embryonic mouse spinal cord. *Neuroreport* 1995, 6:2269–2272
- Zia S, Ndoye A, Lee TX, Webber RJ, Grando SA: Receptor-mediated inhibition of keratinocyte migration by nicotine involves modulations of calcium influx and intracellular concentration. *J Pharmacol Exp Ther* 2000, 293:973–981
- Fucile S, Renzi M, Lauro C, Limatola C, Ciotti T, Eusebi F: Nicotinic cholinergic stimulation promotes survival and reduces motility of cultured rat cerebellar granule cells. *Neuroscience* 2004, 127:53–61
- Sato N, Watanabe S, Hirose M, Wang XE, Maehiro K, Murai T, Kobayashi O, Nagahara A, Ogihara T, Kitami N: Effect of nicotine in migration and proliferation of rabbit gastric mucosal cells in a culture cell model. *J Gastroenterol Hepatol* 1994, 9(Suppl 1):S66–S71
- Drell TL, Joseph J, Lang K, Niggemann B, Zaenker KS, Entschladen F: Effects of neurotransmitters on the chemokinesis and chemotaxis of MDA-MB-468 human breast carcinoma cells. *Breast Cancer Res Treat* 2003, 80:63–70
- Chernyavsky AI, Arredondo J, Marubio LM, Grando SA: Differential regulation of keratinocyte chemokinesis and chemotaxis through distinct nicotinic receptor subtypes. *J Cell Sci* 2004, 117:5665–5679
- Chavez-Noriega LE, Crona JH, Washburn MS, Urrutia A, Elliott KJ, Johnson EC: Pharmacological characterization of recombinant human neuronal nicotinic acetylcholine receptors h alpha 2 beta 2, h alpha 2 beta 4, h alpha 3 beta 2, h alpha 3 beta 4, h alpha 4 beta 2, h alpha 4 beta 4 and h alpha 7 expressed in *Xenopus* oocytes. *J Pharmacol Exp Ther* 1997, 280:346–356
- Papke RL, Duvoisin RM, Heinemann SF: The amino terminal half of the nicotinic beta-subunit extracellular domain regulates the kinetics

- of inhibition by neuronal bungarotoxin. *Proc R Soc Lond B Biol Sci* 1993, 252:141–148
26. Buisson AC, Zahm JM, Polette M, Pierrot D, Bellon G, Puchelle E, Birembaut P, Tournier JM: Gelatinase B is involved in the in vitro wound repair of human respiratory epithelium. *J Cell Physiol* 1996, 166:413–426
27. Lechner JF, LaVeck MA: A serum-free method for culturing normal human bronchial epithelial cells at clonal density. *J Tissue Culture Methods* 1985, 9:43–48
28. Legrand C, Gilles C, Zahm JM, Polette M, Buisson AC, Kaplan H, Birembaut P, Tournier JM: Airway epithelial cell migration dynamics. MMP-9 role in cell-extracellular matrix remodeling. *J Cell Biol* 1999, 146:517–529
29. Buisson AC, Gilles C, Polette M, Zahm JM, Birembaut P, Tournier JM: Wound repair-induced expression of a stromelysins is associated with the acquisition of a mesenchymal phenotype in human respiratory epithelial cells. *Lab Invest* 1996, 74:658–669
30. Zahm JM, Kaplan H, Herard AL, Doriot F, Pierrot D, Somelette P, Puchelle E: Cell migration and proliferation during the in vitro wound repair of the respiratory epithelium. *Cell Motil Cytoskeleton* 1997, 37:33–43
31. Grynkiewicz G, Poenie M, Tsien RY: A new generation of Ca<sup>2+</sup> indicators with greatly improved fluorescence properties. *J Biol Chem* 1985, 260:3440–3450
32. Gerzanich V, Peng X, Wang F, Wells G, Anand R, Fletcher S, Lindstrom J: Comparative pharmacology of epibatidine: a potent agonist for neuronal nicotinic acetylcholine receptors. *Mol Pharmacol* 1995, 48:774–782
33. Wang F, Gerzanich V, Wells GB, Anand R, Peng X, Keyser K, Lindstrom J: Assembly of human neuronal nicotinic receptor alpha5 subunits with alpha3, beta2, and beta4 subunits. *J Biol Chem* 1996, 271:17656–17665
34. Levandoski MM, Lin Y, Moise L, McLaughlin JT, Cooper E, Hawrot E: Chimeric analysis of a neuronal nicotinic acetylcholine receptor reveals amino acids conferring sensitivity to alpha-bungarotoxin. *J Biol Chem* 1999, 274:26113–26119
35. Cartier GE, Yoshikami D, Gray WR, Luo S, Olivera BM, McIntosh JM: A new alpha-conotoxin which targets alpha3beta2 nicotinic acetylcholine receptors. *J Biol Chem* 1996, 271:7522–7528
36. Harvey SC, McIntosh JM, Cartier GE, Maddox FN, Luetje CW: Determinants of specificity for alpha-conotoxin MII on alpha3beta2 neuronal nicotinic receptors. *Mol Pharmacol* 1997, 51:336–342
37. Grant GA, Luetje CW, Summers R, Xu XL: Differential roles for disulfide bonds in the structural integrity and biological activity of kappa-bungarotoxin, a neuronal nicotinic acetylcholine receptor antagonist. *Biochemistry* 1998, 37:12166–12171
38. Martin WR, Brown C, Zhang YJ, Wu R: Growth and differentiation of primary tracheal epithelial cells in culture: regulation by extracellular calcium. *J Cell Physiol* 1991, 147:138–148
39. Mandeville JT, Ghosh RN, Maxfield FR: Intracellular calcium levels correlate with speed and persistent forward motion in migrating neutrophils. *Biophys J* 1995, 68:1207–1217
40. Giannone G, Ronde P, Gaire M, Beaudouin J, Haiech J, Ellenberg J, Takeda K: Calcium rises locally trigger focal adhesion disassembly and enhance residency of focal adhesion kinase at focal adhesions. *J Biol Chem* 2004, 279:28715–28723
41. Arredondo J, Nguyen VT, Chernyavsky AI, Bercovich D, Orr-Urtreger A, Kummer W, Lips K, Vetter DE, Grando SA: Central role of alpha7 nicotinic receptor in differentiation of the stratified squamous epithelium. *J Cell Biol* 2002, 159:325–336
42. Nguyen VT, Hall LL, Gallacher G, Ndoye A, Jolkovsky DL, Webber RJ, Buchli R, Grando SA: Choline acetyltransferase, acetylcholinesterase, and nicotinic acetylcholine receptors of human gingival and esophageal epithelia. *J Dent Res* 2000, 79:939–949
43. Elias JA, Zhu Z, Chupp G, Homer RJ: Airway remodeling in asthma. *J Clin Invest* 1999, 104:1001–1006
44. Fahy JV: Remodeling of the airway epithelium in asthma. *Am J Respir Crit Care Med* 2001, 164:S46–S51
45. Jeffery PK: Remodeling in asthma and chronic obstructive lung disease. *Am J Respir Crit Care Med* 2001, 164:S28–S38
46. Zahm JM, Pierrot D, Chevillard M, Puchelle E: Dynamics of cell movement during the wound repair of human surface respiratory epithelium. *Biorheology* 1992, 29:459–465
47. Flores CM, Rogers SW, Pabreza LA, Wolfe BB, Kellar KJ: A subtype of nicotinic cholinergic receptor in rat brain is composed of alpha 4 and beta 2 subunits and is up-regulated by chronic nicotine treatment. *Mol Pharmacol* 1992, 41:31–37
48. James JR, Nordberg A: Genetic and environmental aspects of the role of nicotinic receptors in neurodegenerative disorders: emphasis on Alzheimer's disease and Parkinson's disease. *Behav Genet* 1995, 25:149–159
49. Wanner A, Salathe M, O'Riordan TG: Mucociliary clearance in the airways. *Am J Respir Crit Care Med* 1996, 154:1868–1902
50. Ayers MM, Jeffery PK: Proliferation and differentiation in mammalian airway epithelium. *Eur Respir J* 1988, 1:58–80
51. Fucile S: Ca<sup>2+</sup> permeability of nicotinic acetylcholine receptors. *Cell Calcium* 2004, 35:1–8
52. Seguela P, Wadiche J, Dineley-Miller K, Dani JA, Patrick JW: Molecular cloning, functional properties, and distribution of rat brain alpha 7: a nicotinic cation channel highly permeable to calcium. *J Neurosci* 1993, 13:596–604
53. Delbono O, Gopalakrishnan M, Renganathan M, Monteggia LM, Messi ML, Sullivan JP: Activation of the recombinant human alpha 7 nicotinic acetylcholine receptor significantly raises intracellular free calcium. *J Pharmacol Exp Ther* 1997, 280:428–438
54. Vernino S, Amador M, Luetje CW, Patrick J, Dani JA: Calcium modulation and high calcium permeability of neuronal nicotinic acetylcholine receptors. *Neuron* 1992, 8:127–134
55. Rogers M, Dani JA: Comparison of quantitative calcium flux through NMDA, ATP, and ACh receptor channels. *Biophys J* 1995, 68:501–506
56. Gerzanich V, Wang F, Kuryatov A, Lindstrom J: Alpha 5 subunit alters desensitization, pharmacology, Ca<sup>++</sup> permeability and Ca<sup>++</sup> modulation of human neuronal alpha 3 nicotinic receptors. *J Pharmacol Exp Ther* 1998, 286:311–320
57. Olale F, Gerzanich V, Kuryatov A, Wang F, Lindstrom J: Chronic nicotine exposure differentially affects the function of human alpha3, alpha4, and alpha7 neuronal nicotinic receptor subtypes. *J Pharmacol Exp Ther* 1997, 283:675–683
58. Mittal AK, Bereiter-Hahn J: Ionic control of locomotion and shape of epithelial cells: I. Role of calcium influx. *Cell Motil* 1985, 5:123–136